

Properties of elliptical-core two-mode fiber

Z. Wang^{a, b}, J. Ju^a, W. Jin^a

^a Department of Electrical Engineering, The Hong Kong Polytechnic University, Kowloon, Hong Kong

^b School of Electronics and Information Engineering, Beijing Jiaotong University, 100044, China
eezwang@polyu.edu.hk

Abstract: Polarization and modal birefringence of elliptical-core two-mode fibers are investigated. Wavelengths corresponding to zero group delay difference (GDD) between the two spatial modes and between the orthogonal polarizations are computed when the fiber parameters, i.e., the relative core/cladding index difference and the ratio of major over minor axis, are varied. Simple relationships between the zero GDD wavelengths and fiber parameters are obtained. With proper fiber design, zero GDD between the two spatial modes and the two orthogonal polarizations can be achieved at the same wavelength.

©2005 Optical Society of America

OCIS codes: (060.2270) Fiber characterization; (060.2280) Fiber design and fabrication; (060.2340) Fiber optics components

References and links

1. S. Ramachandran, "Novel photonic devices in few-mode fibres," *IEE Proc.- Circuits Devices Syst.* **150**, 473-479 (2003).
2. A.M. Vengsarkar, W.C. Michie, L. Jankovic, B. Culshaw, and R.O. Claus, "Fiber-optic dual-technique sensor for simultaneous measurement of strain and temperature," *J. Lightwave Technol.* **12**, 170-177 (1994).
3. H.S. Park, K.Y. Song, S.H. Yun, and B. Y. Kim, "All-fiber wavelength-tunable acoustooptic switches based on intermodal coupling in fibers," *J. Lightwave Tech.* **20**, 1864-1868 (2002).
4. K. Y. Song, and B.Y. Kim, "Broad-band LP01 mode excitation using a fused-typed mode-selective coupler," *IEEE Photon. Technol. Lett.* **15**, 1734-1736 (2003).
5. H.S. Park, S.H. Yun, I.K. Hwang, S.B. Lee, and B.Y. Kim, "All-fiber add-drop wavelength-division multiplexer based on intermodal coupling," *IEEE Photon. Technol. Lett.* **13**, 460-462 (2001).
6. W.V. Sorin, B.Y. Kim, and H.J. Shaw, "Highly selective evanescent modal filter for two-mode optical fibers," *Opt. Lett.* **11**, 581-583 (1986).
7. S.H. Yun, I.K. Hwang, and B.Y. Kim, "All-fiber tunable filter and laser based on two-mode fiber," *Opt. Lett.* **21**, 27-29 (1996).
8. K.A. Murphy, M.S. Miller, A.M. Vengsarkar, and R.O. Claus, "Elliptical-core two-mode optical-fiber sensor implementation methods," *J. Lightwave Technol.* **8**, 1688-1696 (1990).
9. B.Y. Kim, J.N. Blake, S.Y. Huang, and H.J. Shaw, "Use of highly elliptical core fibers for two-mode fiber devices," *Opt. Lett.* **12**, 729-731 (1987).
10. J.N. Blake, S.Y. Huang, B.Y. Kim, and H.J. Shaw, "Strain effects on highly elliptical core two-mode fibers," *Opt. Lett.* **12**, 732-734 (1987).
11. S.Y. Huang, J.N. Blake, and B.Y. Kim, "Perturbation effects on mode propagation in highly elliptical core two-mode fibers," *J. Lightwave Technol.* **8**, 23-33 (1990).
12. K.Y. Song, I.K. Hwang, S.H. Yun, and B.Y. Kim, "High performance fused-type mode-selective coupler using elliptical core two-mode fiber at 1550nm," *IEEE Photon. Technol. Lett.* **14**, 501-503 (2002).
13. J. Ju, W. Jin, and M.S. Demokan, "Two-mode operation in highly birefringent photonic crystal fiber," *IEEE Photon. Technol. Lett.* **16**, 2472-2474 (2004).
14. A.W. Snyder and X.-H. Zheng, "Optical fibers of arbitrary cross sections," *J. Opt. Soc. Am. A* **3**, 600-609 (1986).
15. K. Thyagarajan, S.N. Sarkar, and B.P. Pal, "Equivalent step index (ESI) model for elliptic core Fibers," *J. Lightwave Technol.* **LT-5**, 1041-1044 (1987).
16. Masashi Eguchi, Masanori Koshiba, "Accurate finite-element analysis of dual-mode highly elliptical-core fibers," *J. Lightwave Technol.* **12**, 607-613 (1994).
17. Robert L. Gallawa, I. C. Goyal, Yinggang Tu, and Ajoy K. Ghatak, "Optical waveguide modes: an approximate solution using Galerkin's method with Hermite-Gauss basis functions," *IEEE J. Quan. Electron.* **21**, 518-522 (1991).
18. Tzong-Lin Wu, and Hung-chun Chang, "An efficient numerical approach for determining the dispersion characteristics of dual-mode elliptical-core optical fibers," *J. Lightwave Technol.* **13**, 1926-1934 (1995).
19. R.B. Dyott, *Elliptical Fiber Waveguides*, (Boston, Artech House, 1995).

20. C.D. Poole, J.M. Wiesenfeld, and D.J. Digiovanni, "Elliptical-core dual-mode fiber dispersion compensator," *IEEE Photon. Technol. Lett.* **5**, 194-197 (1993).
 21. C.D. Poole, J.M. Wiesenfeld, D.J. Digiovanni, and A.M. Vengsarkar, "Optical fiber-based dispersion compensation using higher order modes near cutoff," *J. Lightwave Technol.* **12**, 1746-1758 (1994).
 22. Wang Zhi, Ren Guobin, Lou Shuqin, Liang Weijun, "Investigation of the supercell based orthonormal basis function method for different kinds of fibers," *Opt. Fiber Technol.* **10**, 296-311 (2004).
 23. J.D. Joannopoulos, R.D. Meade, J.N. Winn, *Photonic crystals: molding the flow of light*, (New York, Princeton university press, 1995).
 24. J. Blake, M.C. Pacitti, S.L.A. Carrara, "Splitting of the Second Order Mode Cutoff Wavelengths in Elliptical Core Fibers," *Optical Fiber Sensors Conference*, 1992. 8th, Jan. 29-31, 125-128 (1992).
-

1. Introduction

Two-mode optical fibers have been studied for a number of devices and sensors applications [1-13]. Two-mode operation can be achieved by operating a conventional circular-core fiber below cut-off and hence it supports the fundamental LP_{01} and the second order hybrid LP_{11} modes. The performance of these devices is however not stable because the hybrid LP_{11} is actually consists of four true modes that have slightly different propagation constants and coherent mixing of these modes results in variation of the hybrid mode intensity pattern along the fiber length and with environmental disturbance. The same applies to the polarization states of the fundamental mode. These problems can be overcome by elliptical core fibers [5-10]. In an elliptical core fiber, the hybrid LP_{11} mode split into two groups, i.e., LP_{11} odd and LP_{11} even modes, with well defined mode intensity patterns. The LP_{11} odd and LP_{11} even modes have significantly different cut off wavelengths, which allows the existence of a wavelength range within which only LP_{01} and LP_{11} even modes are supported by the fiber.

The elliptical-core fibers that support two stable spatial modes, i.e., the LP_{01} and LP_{11} even modes, are named elliptical-core two-mode fibers. The applications of these fibers include interferometric modal/polarimetric sensors that can be used to measure strain, temperature or both at the same time [2,8-10]. The performances of the interferometric systems are affected by two important parameters, i.e., the group delay difference (GDD) and the phase delay difference (PDD) between the two spatial modes or between the two orthogonal polarizations of the same spatial mode. For example, in a two-mode fiber interferometer in which the GDD between two modes can be designed to approximately zero, a light source with a short coherence length can be used without losing interference signals even though large PDD between the two modes may be employed [9]. There are some analyses about the elliptical-core two-mode fibers, which paid attention to modeling the dispersion properties [14-22] of the x- and y- components of the fundamental mode (LP_{01}^x , LP_{01}^y) and the dispersion properties of the second order even mode (LP_{11} even) near cutoff. However, to the best of our knowledge, little or no effort has been made to study the group delay difference between the two well-confined (away from cutoff) spatial modes as functions of fiber parameters, which are important for optimizing the performance of two mode interferometers.

In this paper, we study the modal behavior of step-index elliptical-core two-mode fibers, with emphases on the group delay difference between the two confined spatial modes, and the dependence of the characteristic wavelengths on the fiber structural parameters, (i.e., the cutoff wavelengths of the LP_{11} even and odd modes, the wavelength corresponding to zero-GDD between two spatial modes and between two orthogonal polarizations of the same spatial mode), which is believed to be useful for designing fiber for interferometer sensor applications. The relationship between zero-GDD wavelengths of the two orthogonal polarizations of both LP_{01} and LP_{11} even modes and the fiber parameters are presented in Section 2; the properties of the two-mode elliptical core fibers, including the cutoff wavelength of the even and odd LP_{11} modes, the zero-GDD wavelength between the two spatial modes and the modal beat length at this wavelength are presented in Section 3; a particular fiber, which has the same zero-GDD wavelength for the two orthogonal polarizations of the fundamental mode and for the two spatial modes, is presented in Section 4.

2. Zero GDD wavelength for two orthogonal polarizations

Figure 1(a) shows the cross-section of a step index elliptical-core fiber (ECF), which is characterized by three parameters: a , the semi major axis; b , the semi minor axis; and Δ , the core-cladding relative refractive index difference. The polarization modal birefringence (PMB) $\Delta\beta$, which is defined as the difference between the propagation constants of the orthogonal polarization components of the mode (i.e., $\Delta\beta_{PMB1}$ between LP_{01}^x and LP_{01}^y , $\Delta\beta_{PMB2}$ between LP_{11}^x even and LP_{11}^y even), tends to zero at both short and long wavelengths and reaches its maximum value at an intermediate wavelength [19]. Take the elliptical-core fiber with the structural parameters of $a=3\mu\text{m}$, $\Delta=0.5\%$, and the aspect ratio $\eta=a/b=2.5$, as an example, $\Delta\beta$ and the GDD between both polarization components of both LP_{01} and LP_{11} even modes are plotted in Fig. 1(b). At λ_{MPMB1} , $\Delta\beta_{PMB1}$ reaches its maximum, the GDD between the two orthogonal polarizations of LP_{01} mode, i.e.,

$$\Delta\tau_{gp} = d(\Delta\beta_{PMB1})/d\omega = -\frac{\lambda^2}{2\pi c} \frac{d(\Delta\beta_{PMB1})}{d\lambda}, \quad (1)$$

equals to zero, where c is the light velocity in vacuum. Hence λ_{MPMB1} is also the wavelength (λ_{0p1}) at which the GDD between the two orthogonal polarizations is zero.

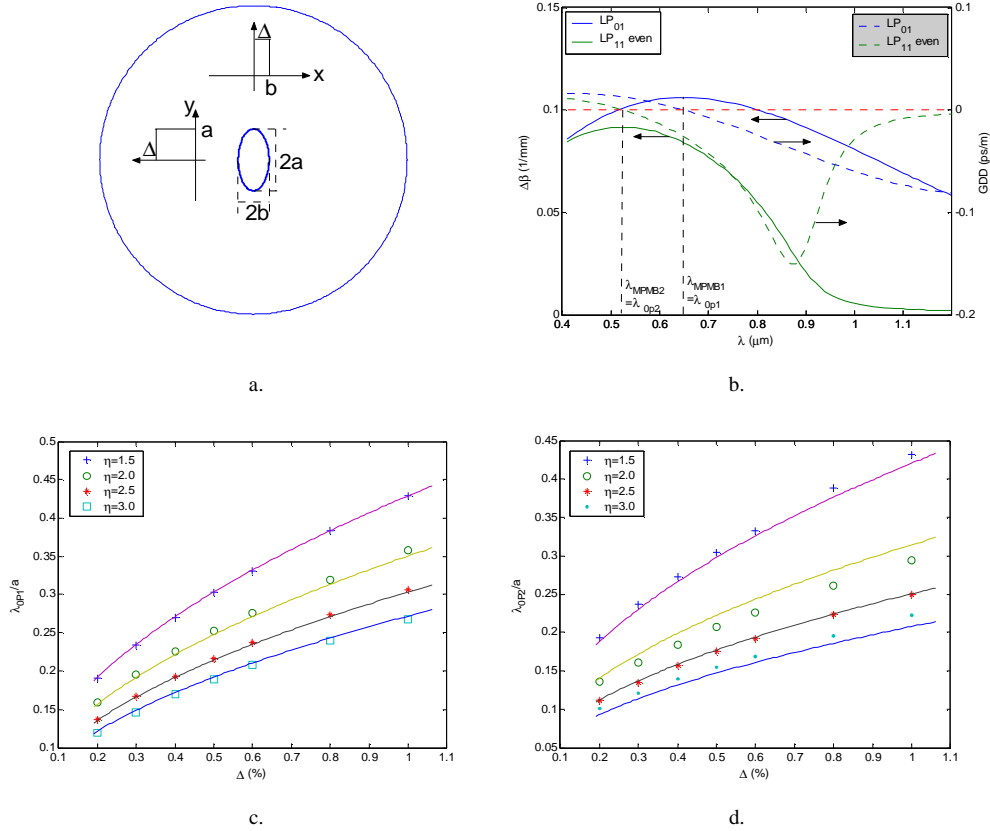


Fig.1. (a) The cross-section of the elliptical-core fiber; (b) $\Delta\beta$ and GDD of an ECF with structural parameters of $a=3\mu\text{m}$, $\Delta=0.5\%$, $\eta=2.5$; (c) the relationship between λ_{0p1} and fiber parameters; (d) the relationship between λ_{0p2} and fiber parameters.

Figure 1(c) shows the relationship between λ_{0p1} and Δ for different aspect ratio η . The data points '+', 'o', '*' and '□' are the results from numerical calculations using a super-cell

method [22]. The four lines are plotted by using Eq. (2a), which is fitted from the numerical results.

From Fig. 1(b), it can also be seen that $\Delta\beta_{\text{PMB2}}$ reaches its maximum at an intermediate wavelength λ_{MPMB2} which is also the wavelength λ_{OP2} at which the GDD between the two orthogonal polarizations of the LP₁₁ even mode is zero. The relationship between the wavelength λ_{OP2} and fiber structure parameters can also be fitted to a simple form as given by Eq. (2b). The numerical and the fitted results are plotted in Fig. 1(d) as data points and lines.

$$\frac{\lambda_{\text{OP1}}}{a} = \frac{\lambda_{\text{MPMB}}}{a} = \left(\frac{C_1}{\eta} + C_2 \right) \sqrt{\Delta}, \quad C_1 \approx 4.714, \quad C_2 \approx 1.148. \quad (2a)$$

$$\frac{\lambda_{\text{OP2}}}{a} = \frac{\lambda_{\text{MPMB2}}}{a} = \left(\frac{C'_1}{\eta} + C'_2 \right) \sqrt{\Delta}, \quad C'_1 \approx 6.390, \quad C'_2 \approx -0.05194. \quad (2b)$$

Based on the scaling property of the Maxwell's equations [23], the wavelength in Fig.1(c), (d) and in Eq.(2) are normalized to the semi major axis (a) of the elliptical core and should be applicable to any value of a . λ_{OP1} (λ_{MPMB1}) and λ_{OP2} (λ_{MPMB2}) are proportional to $\Delta^{1/2}$. The results obtained from Eq. (2) have good agreement with those reported by others [16,19], which is helpful for designing an ECF to achieve the max-PMB at a particular wavelength.

3. properties of two-mode fibers

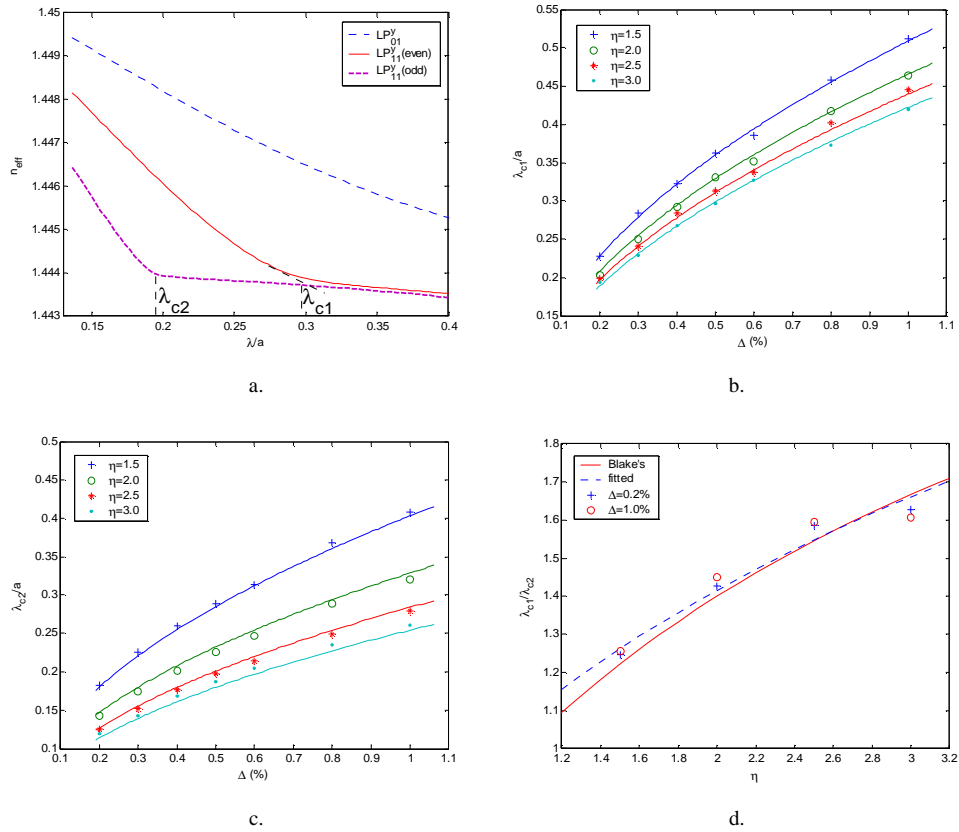


Fig. 2. (a) The effective mode index of an ECF with the parameters same as given in Fig. 1(b); (b) and (c) the numerical and fitted results of the cutoff wavelengths of LP₁₁ even and LP₁₁ odd modes; (d) the ratio of the even to odd LP₁₁ mode cutoff wavelengths as a function of aspect ratio.

The splitting of the cutoff wavelengths of LP₁₁ even and odd modes, shown as λ_{c1} and λ_{c2} in Fig. 2(a), has been reported by J. Blake et al. [24]. The beat length between the first and second order spatial modes, and the wavelength at which the first and second order spatial modes propagated with the same group velocity have however not been accurately predicted to our knowledge. These calculations are much more difficult than predicting the general modal behavior because the results depend on the difference in propagation constants between two spatial modes.

3.1 cutoff wavelengths of LP₁₁ even and LP₁₁ odd modes

Figure 2(a) shows the effective mode index (n_{eff}) of the y-polarization of three lowest-order modes (LP₀₁, LP₁₁ even, LP₁₁ odd) of an ECF with the same parameters as given in Fig. 1(b). λ_{c1} and λ_{c2} are the cutoff wavelength of LP₁₁ even and LP₁₁ odd modes, respectively. The ECF will support two modes (LP₀₁ and LP₁₁ even) within the wavelength range of from λ_{c2} to λ_{c1} .

Figure 2(b) and 2(c) shows the dependences of λ_{c1} and λ_{c2} on the fiber parameters (Δ and η), respectively. Again, the data points are numerically computed values and the lines are the fitted curves of according to Eq. (3a) and (3b), respectively.

$$\frac{\lambda_{c1}}{a} = \left(\frac{C_3}{\eta} + C_4 \right) \sqrt{\Delta}, \quad C_3 \approx 2.602, \quad C_4 \approx 3.356, \quad (3a)$$

$$\frac{\lambda_{c2}}{a} = \left(\frac{C'_3}{\eta} + C'_4 \right) \sqrt{\Delta}, \quad C'_3 \approx 4.474, \quad C'_4 \approx 1.051, \quad (3b)$$

For comparison, the ratio of λ_{c1} to λ_{c2} calculated from Eq. (3) and that obtained from ref. [24] are plotted in Fig. 2(d), where the numerical results of $\Delta=0.2\%$ and $\Delta=1\%$ are also plotted. It shows that the fitted expressions have a good agreement with Ref. [24].

3.2 zero-GDD wavelength

In a two-mode fiber, GDD ($\Delta\tau_{gs}$) and PDD ($\Delta\tau_{ps}$) between the two spatial modes per fiber length can be expressed as

$$\Delta\tau_{gs} = d(\Delta\beta_{SMB})/d\omega = -\frac{\lambda^2}{2\pi c} \frac{d(\Delta\beta_{SMB})}{d\lambda}, \quad (4a)$$

$$\Delta\tau_{ps} = \Delta\beta_{SMB}/\omega = \frac{\Delta\beta_{SMB}}{2\pi c} \lambda, \quad (4b)$$

where $\Delta\beta_{SMB}=\beta_{01}-\beta_{11}$ is called spatial mode birefringence (SMB); β_{01} and β_{11} are the propagation constants of LP₀₁ mode and LP₁₁ even mode, respectively.

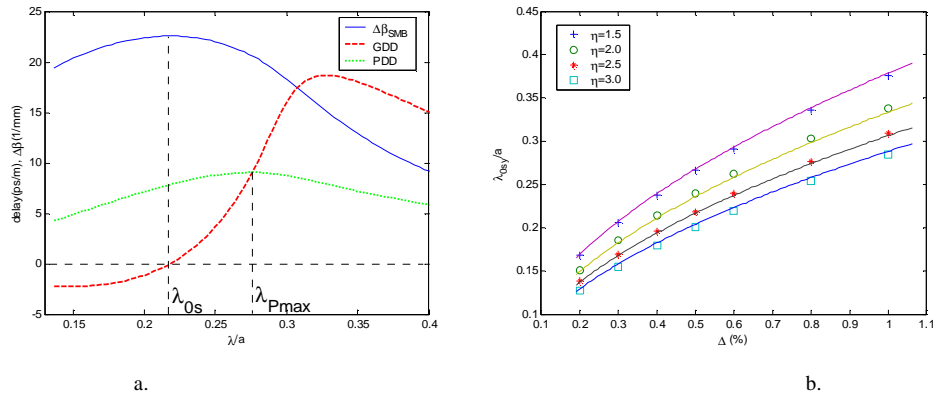


Fig. 3. (a) The GDD, PDD and the SMB of an ECF with the same parameters as given in Fig. 1(b), (b) The relationship between zero-GDD wavelength λ_{0s} and the fiber parameters η and Δ .

In general, $\Delta\tau_{gs}$, $\Delta\tau_{ps}$ and $\Delta\beta_{SMB}$ are all polarization dependent. The GDD, PDD and SMB between the y polarization components of the two spatial modes for the ECF with parameters given in Fig. 1(b) are plotted in Fig. 3(a). As expected, the wavelength λ_{0s} where the GDD is zero equals to the wavelength λ_{MSMB} where $\Delta\beta_{SMB}$ is maximized, and the GDD equals to the PDD at the wavelength λ_{Pmax} where PDD is maximized.

Figure 3(b) shows the relationship between λ_{0sy} (subscript ‘y’ represents the y polarization component) and Δ for various values of η . Again, the data points are obtained from numerical calculation and are fitted into a simple formula given in Eq. (5a). The four lines are obtained from Eq. (5a) and agree well with the numerical results. Eq. (5b) shows the fitted form of the zero-GDD wavelength of the x-components between LP₀₁ and LP₁₁ even modes. It is obvious that there is only a little difference between the results for the orthogonal polarization components.

$$\frac{\lambda_{0sy}}{a} = \frac{\lambda_{MSMB_y}}{a} = \left(\frac{C_5}{\eta} + C_6 \right) \sqrt{\Delta}, \quad C_5 \approx 2.710, C_6 \approx 1.981, \quad (5a)$$

$$\frac{\lambda_{0sx}}{a} = \frac{\lambda_{MSMB_x}}{a} = \left(\frac{C'_5}{\eta} + C'_6 \right) \sqrt{\Delta}, \quad C'_5 \approx 2.732, C'_6 \approx 1.966. \quad (5b)$$

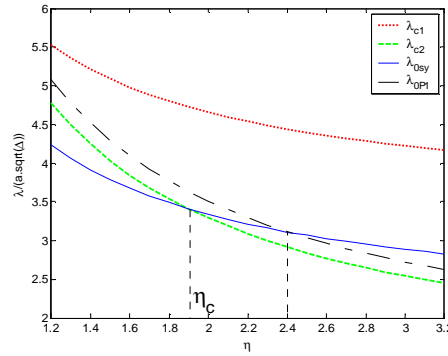


Fig. 4. Comparison of λ_{c1} , λ_{c2} , λ_{0sy} and λ_{0p1}

From Eqs. (3) and (5), it can be found that the zero-GDD wavelength is outside the two-mode range, i.e., $\lambda_{0s} < \lambda_{c2}$, when η is less than ~ 1.90 . Fig. 4, in which $\lambda/(a \sqrt{\Delta})$ are plotted from Eq. (2), Eq. (3) and Eq. (5), also demonstrates the critical value of the aspect ratio $\eta_c \approx 1.90$. This means that the first and second order modes can not propagate with the same group velocity in a two-mode ECF with $\eta < 1.90$. From Fig. 4, it can also be seen that the zero GDD between the two spatial modes and the zero GDD (or maximum birefringence) between the orthogonal polarizations of the fundamental modes can be achieved at the same wavelength ($\lambda_{0s} = \lambda_{0p1}$) at $\eta \approx 2.4$. This will be further discussed in section 4.

3.3 beat length at zero-GDD wavelength

Polarization and modal beat lengths are important parameters for polarimeters and modal interferometers. In a two-mode elliptical core fiber, four possible interferometers may be implemented, i.e., polarimeters formed between the orthogonal polarizations of the LP₀₁ and LP₁₁ even modes; and modal interferometers formed between the LP₀₁ and LP₁₁ even modes for each of the orthogonal polarizations. Hence, four beat lengths, i.e., polarization beat length for LP₀₁ mode ($L_{PMB1} = 2\pi/\Delta\beta_{PMB1}$), the polarization beat length for LP₁₁ even mode ($L_{PMB2} = 2\pi/\Delta\beta_{PMB2}$), the spatial modal beat length ($L_{SMB_y} = 2\pi/\Delta\beta_{SMB_y}$) for the y-polarization component, and the spatial modal beat length ($L_{SMB_x} = 2\pi/\Delta\beta_{SMB_x}$) for the x-polarization component, need to be considered for the corresponding interferometers. Figs. 5(a), 5(b) and 5(c) show respectively L_{PMB1} , L_{PMB2} and L_{SMB_y} at zero-GDD wavelength λ_{0s} as functions of Δ

for various values of η . The data points are obtained from numerical calculations and the lines are fitted results according to Eqs. (6a), (6b) and (6c).

$$\frac{L_{PMB1}}{a} = \frac{C_7}{\eta^2 \Delta^{3/2}}, C_7 \approx 44.18, \quad (6a)$$

$$\frac{L_{PMB2}}{a} = \frac{C_8}{(\eta^2 + C_9) \Delta^{3/2}}, C_8 \approx 4.163, C_9 \approx -1.286, \quad (6b)$$

$$\frac{L_{SMBy}}{a} = \frac{C_{10} \eta + C_{11}}{\sqrt{\Delta}}, C_{10} \approx 0.22, C_{11} \approx 6.0. \quad (6c)$$

$$\frac{1}{L_{SMBx}} - \frac{1}{L_{SMBy}} = \frac{1}{L_{PMB2}} - \frac{1}{L_{PMB1}}. \quad (6d)$$

The beat length L_{SMBx} is not shown because it is not an independent quantity and can be obtained from the other three beat lengths through Eq. (6d). The polarization modal beat lengths (L_{PMB1} and L_{PMB2}) have $\Delta^{-3/2}$ dependence, and the spatial modal beat lengths (L_{SMBy} and L_{SMBx}) have a $\Delta^{-1/2}$ dependence.

In design two-mode interferometers based on elliptical-core fibers, the properties of the fiber, including the two-mode wavelength range, the zero-GDD wavelengths and the beat lengths at these wavelengths, can be estimated from Eqs. (3), (5) and (6), respectively, and hence the performance of the interferometer.

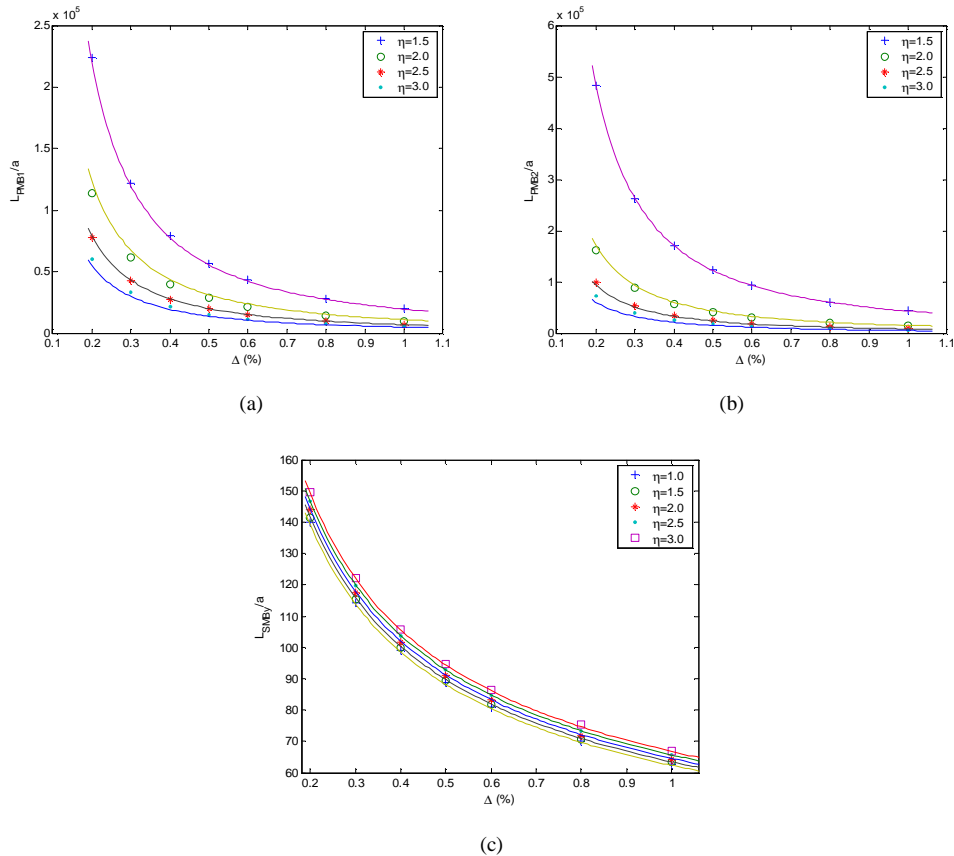


Fig. 5. The relationship between the beat length (a: L_{PMB1} , b: L_{PMB2} , c: L_{SMBy}) at λ_{0s} and Δ for various η .

4. A particular elliptical core fiber

From Eqs. (2) and (5), or Fig. 4, it can be seen that λ_{MPMB1} (i.e., λ_{0P1}) equals to λ_{MSMB} (i.e., λ_{0S}) when $\eta \approx 2.4$. Fibers satisfy this condition can have zero GDD between the two orthogonal polarizations and the two spatial modes at the same wavelength of $\lambda_0 \approx 3.11a \cdot \text{sqrt}(\Delta)$. Fig. 6 shows the $\Delta\beta_{\text{PMB1}}$, $\Delta\beta_{\text{SMBY}}$ and GDD as function of wavelength for a particular elliptical-core fiber with $\eta=2.4$, $a=5\mu\text{m}$, $\Delta=1\%$. This fiber has a zero-GDD wavelength for both polarizations and spatial modes at around $1.55\mu\text{m}$. The zero-GDD wavelengths (λ_{0sy} and λ_{MPMB1}), the spatial modal beat length and the polarization modal beat length at λ_{0sy} , are presented in Table 1. The difference between the results obtained numerically and those obtained from the fitted formulas compared well with errors given in the last column of the table. The value of λ_{0sx}/a , which is not listed in the table, equals to 0.310434 and is very close to λ_{0sy} .

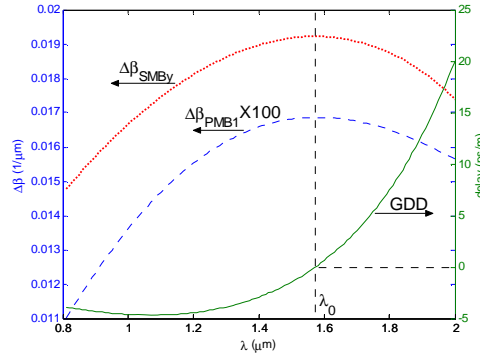


Fig. 6. The PMB, SMB and GDD of a two-mode ECF with the structural parameters $a=5\mu\text{m}$, $\eta=2.4$, $\Delta=0.01$. The PMB is amplified by 100 times in order to be plotted with the SMB.

Table 1. The fitted and the numerical results of a two-mode ECF with $a=5\mu\text{m}$, $\eta=2.4$, $\Delta=0.01$.

	fitted	numerical	Errors
$\lambda_{\text{0sy}}/a = \lambda_{\text{MSMB}}/a$	0.311066	0.314912	1.2287%
$\lambda_{\text{0p1}}/a = \lambda_{\text{MPMB1}}/a$	0.311216	0.315200	1.2718%
$L_{\text{PMB2}}/a @ \lambda_{\text{0s}}$	9304.872	9628.053	3.4140%
$L_{\text{PMB1}}/a @ \lambda_{\text{0s}}$	7670.138	7447.658	2.9430%
$L_{\text{SMBY}}/a @ \lambda_{\text{0s}}$	65.280	65.346	0.1010%
$L_{\text{SMBX}}/a @ \lambda_{\text{0s}}$	65.378	65.476	0.1498%

5. Conclusion

In conclusion, the modal properties of the step-index elliptical-core two-mode fibers are investigated. It is found that the wavelengths corresponding to zero GDD between the two spatial modes and between the orthogonal polarization components, and the polarization and modal beat lengths at the zero GDD wavelengths have simple relationships with the aspect ratio η and relative core/cladding refractive index Δ . These relationships can be used to design two-mode fibers and two-mode fiber interferometers with optimized performance.

Acknowledgments

This project is supported by the government of the Hong Kong Special Administrative Region of China through a CERG grant- PolyU 5207/03E, and by the National Natural Science Foundation Project of China (grant No. 60402006).